A synthetic analogue of melittin aggregates in large oligomers

Edgar John and Fritz Jähnig
Max-Planck-Institut für Biologie, D-7400 Tübingen, Germany

ABSTRACT An analogue of melittin synthesized in the group of E. T. Kaiser (DeGrado, W. F., F. J. Kezdy, and E. T. Kaiser. 1981. *J. Am. Chem. Soc.* 103:679–681) was investigated by Raman spectroscopy and fluorescence anisotropy decay. In water, the analogue is completely α-helical and aggregates in large oligomers of about 50 monomers. In vesicle membranes, it undergoes orientational fluctuations similar to melittin. The most significant difference from melittin, therefore, is the formation of straight helixes and their aggregation in large oligomers in water. We interpret this as a consequence of the lacking proline residue in the analogue. We, furthermore, hypothesize that the increased tendency for aggregation causes the increased hemolytic activity of the analogue.

INTRODUCTION

About 10 years ago, E. T. Kaiser and his co-workers became engaged in assessing the role of the amphiphilic α-helix as a structural feature that effects or improves the binding of peptides and proteins to amphiphilic surfaces (1–4). For this purpose, they designed nonhomologous analogues of amphiphilic α-helixes that had been proposed to occur in peptides or proteins and to serve a special function. The analogues were synthesized and tested for their function to find out whether it was altered or not.

One of the peptides that Kaiser and co-workers decided to work on was melittin, the main component of bee venom (3, 4). Melittin, depicted in Table 1, consists of 26 amino acid residues the NH_2-terminal 20 of which show the pattern of an amphiphilic α-helix, while the 6 residues at the COOH-terminus are strongly hydrophilic. The amphiphilic α-helix is actually formed upon tetramerization in water and upon binding to membranes (for a review, see reference 5). In the former case, two pairs of antiparallel helixes pack crosswise on top of each other, with the hydrophobic sides facing the interior (6). In the latter case, the helixes may either lie flat on the membrane surface or insert into the membrane upon aggregation (7–10). The action of melittin on membranes may be subdivided into two classes, depending on concentration. At low concentration, melittin induces ion channel activity, at high concentration it leads to hemolysis and micellation of membranes. Recently, a molecular model for hemolysis has been proposed (11). Pairs of antiparallel helixes would line up on the membrane surface forming "rafts," which upon interaction would dip into the membrane and thus form large channels. These channels may permit proteins such as hemoglobin to cross the membrane leading to cell lysis. In the case of micellation, the membrane is completely destroyed (12). The amphiphilic α-helixes are supposed to form rings around regions of lipid and thus cut the membrane into disc-shaped micelles.

Kaiser and co-workers asked themselves if the functions of melittin are consequences of the formation of an amphiphilic α-helix. Therefore, they synthesized an analogue with the ability still to form an amphiphilic α-helix over the NH_2-terminal 20 residues, but without any sequence homology to melittin (apart from the Trp residue at position 19) (3). The COOH-terminal hydrophilic segment was retained as such (Table 1). Physicochemical studies of this analogue, called peptide 1, indicated that it resembled melittin in structural aspects such as α-helix content or aggregation in water, and in functional aspects such as hemolysis. However, slight differences were also detectable. The α-helix content of peptide 1 was higher than that of melittin, as might have been expected from the lack of the helix-breaking proline residue at position 14. Somewhat unexpected was the observation that peptide 1 was even more effective in hemolysis than melittin, the concentration required for 50% lysis being lower by about a factor of two.

More recently, another analogue of melittin has been synthesized in which only the proline residue at position 14 was replaced by alanine (13). It was called P14A. To the extent that the structural and functional differences between melittin and peptide 1 are caused by the lacking proline residue, the analogue P14A should behave like peptide 1. Indeed, P14A was found to be α-helical throughout the amphiphilic region (14). The hemolytic effect was found to be twice as strong as for melittin, in consonance with peptide 1. The ion channel activity of P14A was reduced compared to melittin and the process of micellization slowed down.

In the present study, the physicochemical investigations of peptide 1 are extended. The α-helix content of peptide 1 in water is determined by Raman spectroscopy and the degree of aggregation is determined by fluorescence anisotropy decay (FAD). The dynamics of peptide 1 in lipid membranes is also investigated by FAD. Such studies have been performed previously on melittin (15, 16). The most significant difference between

This paper is dedicated to the memory of Prof. E. T. Kaiser.

Address correspondence to Dr. Fritz Jähnig, Abteilung Membranbiochemie, Max-Planck-Institut für Biologie, Corrensstrasse 38, D-7400 Tübingen, Germany.

Dr. John's present address is Ciba-Geigy, K-127.5.20, CH4002 Basel, Switzerland.

0006-3495/92/12/1536/08 $2.00

TABLE 1 **Amino acid sequences of melittin, peptide 1, and δ-hemolysin**

Number	1				5					10					15					20					25		
Melittin	G	I	G	A	V	L	K	V	L	T	T	G	L	P	A	L	I	S	W	I	K	R	K	R	Q	Q	
Peptide 1	L	L	Q	S	L	L	S	L	L	Q	S	L	L	S	L	L	L	Q	W	L	K	R	K	R	Q	Q	
δ-Hemolysin	M	A	Q	D	I	I	S	T	I	G	D	L	V	K	W	I	I	D	T	V	N	K	F	T	K	K	

peptide 1 and melittin is found in the stronger tendency for aggregation of peptide 1 in water. We hypothesize that this stronger aggregation causes the enhanced hemolytic activity of peptide 1 compared to melittin.

MATERIALS AND METHODS

Chemicals

Dimyristoylphosphatidylcholine (DMPC) was purchased from Fluka (Neu-Ulm, Germany) and used without further purification. Para-terphenyl (PTP) was from Sigma (München, Germany) and phenanthrene from Serva (Heidelberg, Germany). All solvents were from Merck (Darmstadt, Germany) and were of spectroscopic grade. The melittin analogue, peptide 1, was a generous gift of Prof. E. T. Kaiser (The Rockefeller University, New York). Synthesis and purification of peptide 1 have been described (3).

Sample preparation

For Raman measurements, 1 mg of peptide 1 was dissolved in 10 μl of distilled water, yielding a peptide concentration of 35 mM. The solution was sealed in a glass capillary. For FAD measurements on peptide 1 in water, a 20 μM solution of the peptide in buffer (10 mM potassium hydrogen phosphate, pH 7.4) was used. The solution was filled in 1 × 1 cm quartz cuvettes.

For FAD measurements on peptide 1 in lipid vesicle membranes, DMPC was dissolved in chloroform and the solvent evaporated under a stream of nitrogen. Buffer (10 mM potassium hydrogen phosphate, pH 7.4) was added to obtain a lipid concentration of 12 mM, then the sample was sonicated in a bath sonicator for 30 min followed by incubation for 2 h at 36°C. Peptide 1 in the same buffer was added to obtain a final lipid concentration of 3 mM and a peptide/lipid mole ratio of 1/150. Before starting a series of FAD measurements, the samples were cooled below the lipid phase transition at 24°C and warmed up to 36°C to avoid any hysteresis effect of the phase transition. After finishing the measurements, the size and shape of the vesicles were controlled by electron microscopy. Almost all vesicles were unilamellar, with diameters between 50 and 200 nm.

The sample used as fluorescence standard was a 5 μM solution of PTP in cyclohexane and the sample used as anisotropy standard was a 160 μM solution of phenanthrene in cyclohexane.

To each sample, a control sample was prepared without the fluorophore.

Raman measurements

The Raman measurements and data analysis were performed as described previously for melittin (15). The sample was irradiated with the 514.5-nm line of an Ar ion laser, the light intensity at the sample being 100 mW. The slit width of the double monochromator was set at 5 cm^{-1}. The scan speed was 1 step per s with a step size of 0.2 Å. Typically, 100 scans across the region of the amide I band between 1500 and 1800 cm^{-1} were recorded. After every 10 scans, 1 scan across the water band between 2,800 and 3,400 cm^{-1} was recorded. The intensity of this water band was used as a scaling factor for the contribution of the weak water band around 1,635 cm^{-1} to the measured spectrum. Its contribution was subtracted. The fluorescence background was about 10 times higher than the amide I band, but was relatively smooth, so that it could be subtracted as a flat baseline yielding the amide I spectrum of the peptide.

For the data analysis in terms of secondary structure of the peptide, the second method of Williams (17) was used with 15 reference proteins and $k_{rank} = 7$. The percentages of secondary structure classes are obtained with an error of ±4%. If one class dominates strongly, the error may become as large as ±15%.

FAD measurements

The FAD measurements and data analysis were performed as described previously for melittin (16). A mode-locked Ar ion laser synchronously pumps a cavity-dumped dye laser to generate light pulses at a repetition rate of 8 MHz. To excite Trp fluorescence, we used Rhodamin 590 (Exciton Chemical Co. Inc., Dayton, OH) as laser dye and set the wavelength of the exciting light, after frequency doubling, at λ_{ex} = 300 nm. The emission wavelength was selected by a monochromator, slit width 8 nm, and a cutoff filter as λ_{em} = 360 nm.

An FAD measurement of one selected sample involved measurements on that selected sample, as well as the control sample, the fluorescence standard sample, and the control sample for the fluorescence standard. The measured intensities of the samples were corrected for background by subtracting the intensities of the control samples. The intensities thus obtained were deconvoluted, using the fluorescence standard. This yielded the intensities $I_\parallel(t)$ and $I_\perp(t)$ of the fluorescence light polarized parallel and perpendicular to the exciting light. The total intensity or sum and the difference were obtained as $S = I_\parallel + 2\beta I_\perp$ and $D = I_\parallel - \beta I_\perp$, with the correction factor $\beta = 1.03 \pm 0.01$. They were fitted by assuming analytical expressions for the sum

$$s(t) = \sum_{i=1}^{N} a_i e^{-t/\tau_i} \tag{1}$$

and the anisotropy

$$r(t) = \sum_{i=1}^{M} b_i e^{-t/\Phi_i} + r_\infty \tag{2}$$

so that $d(t) = r(t)s(t)$. The partial amplitudes α_i of the sum, the average lifetime $\bar{\tau}$, the initial anisotropy r_0, and the average relaxation time $\bar{\Phi}$ are obtained as

$$\begin{aligned} \alpha_i &= a_i \Big/ \sum_{j=1}^{N} a_j \\ \bar{\tau} &= \sum_{i=1}^{N} \alpha_i \tau_i \\ r_0 &= \sum_{i=1}^{M} b_i + r_\infty \\ \bar{\Phi} &= \sum_{i=1}^{M} b_i \Phi_i \Big/ \sum_{i=1}^{M} b_i. \end{aligned} \tag{3}$$

In the case of one fluorescence transition and one relaxation process, the initial and residual anisotropies r_0 and r_∞ can be analyzed in terms of the angles Θ_a and Θ_e of the absorption and emission dipole moments

relative to the symmetry axis of the fluorophore and of the orientational order parameter $\langle P_2 \rangle$ of the fluorophore axis

$$r_0 = {}^2/_5 P_2(\cos(\Theta_a - \Theta_e)) \quad (4)$$

$$r_\infty = {}^2/_5 P_2(\cos\Theta_a) P_2(\cos\Theta_e) \langle P_2 \rangle^2. \quad (5)$$

Here, $P_2(\cos\Theta) = (3\cos^2\Theta - 1)/2$ denotes the second order Legendre polynomial.

As shown previously for melittin, the anisotropy of the Trp fluorescence at long times requires a more sophisticated analysis (16). To compare with melittin, we introduced the same assumptions, namely that two fluorescence transitions exist, a fast and a slow one with $\tau_f < \tau_s$, and that the absorption dipole moments of both fall into the symmetry axis of the fluorophore, $\Theta_{af} = \Theta_{as} = 0$. Then the anisotropy is given by the expression

$$r(t) = \frac{\alpha_f e^{-t/\tau_f} P_2(\cos\Theta_{ef}) + \alpha_s e^{-t/\tau_s} P_2(\cos\Theta_{es})}{\alpha_f e^{-t/\tau_f} + \alpha_s e^{-t/\tau_s}} \cdot \left[\sum_{i=1}^{M} \beta_i e^{-t/\Phi_i} + \beta_{M+1} \right] \quad (6)$$

with $\beta_{M+1} = {}^2/_5 \langle P_2 \rangle^2$ and the normalization condition $\sum_{i=1}^{M+1} \beta_i = {}^2/_5$. The initial and final anisotropies result as

$$r_0 = {}^2/_5 [\alpha_f P_2(\cos\Theta_{ef}) + \alpha_s P_2(\cos\Theta_{es})] \quad (7)$$

$$r_\infty = {}^2/_5 P_2(\cos\Theta_{es}) \langle P_2 \rangle^2. \quad (8)$$

In the analysis of the anisotropy of the Trp fluorescence of peptide 1 in vesicle membranes, we attributed the same emission dipole angle Θ_{ef} to the three short lifetime components and the angle Θ_{es} to the fourth long lifetime component.

RESULTS

Raman spectroscopy on peptide 1 in water

The Raman spectrum in the range 1,500–1,800 cm^{-1} of peptide 1 in water is shown in Fig. 1 *A*. The peptide concentration is 100 mg/ml or 30 mM, hence by analogy to melittin the peptide is expected to be aggregated. The strong band around 1,650 cm^{-1} represents the amide I band, while the band around 1,550 cm^{-1} represents a Trp band. The position of the amide I band at 1,650 cm^{-1} indicates a high α-helix content of peptide 1.

For a quantitative analysis, the amide I band was fitted by a superposition of the spectra of 15 reference proteins as shown in Fig. 1 *B*. From this fit, the percentages of secondary structure classes were obtained as listed in Table 2. For comparison, the data for melittin and polyglycine in water were included. Peptide 1 has an α-helix content of nearly 100%. In this case, the percentages of the other structure classes should vanish. Actually, they are finite but compensate each other. Their finite size is an artefact of the analysis that occurs in the same manner for polyglycine. Hence, the result of the Raman studies is that peptide 1 is completely α-helical. Under the same conditions, melittin has an α-helix content of only 75%.

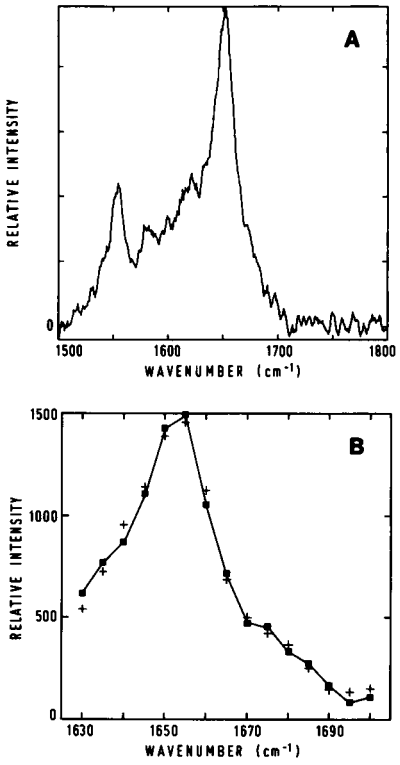

FIGURE 1 (*A*) The Raman amide I band of 1.0 mg peptide 1 in 10 μl water at 20°C. (*B*) 15-point representation of the amide I band of peptide 1 together with the fit by a superposition of the amide I bands of 15 reference proteins (+).

FAD measurements on peptide 1 in water

Fig. 2 shows the intensity and anisotropy of the Trp fluorescence of peptide 1 at a concentration of 20 μM in buffer at low ionic strength. Under these conditions, melittin would be monomeric. The results of fits of the intensity and anisotropy by sums of exponentials are listed in Table 3.

For the intensity, a good fit was obtained by using three exponentials. The three lifetimes are in good agreement with earlier findings for melittin (16, 18). The corresponding amplitudes, however, differ somewhat from the case of melittin in being larger for the short lifetime. Therefore, the mean lifetime of peptide 1 results as τ = 1.9 ns, while monomeric melittin has a mean lifetime of τ = 3.0 ns (16). The value for peptide 1 is closer to the mean lifetime τ = 2.3 ns of tetrameric melittin.

When the anisotropy was fitted by two exponentials, a short relaxation time, Φ_1 = 1.8 ns, and long one, Φ_2 = 78 ns, were obtained. Inclusion of a third exponential did not alter the result, the short relaxation time was simply found twice. By contrast, melittin exhibited a subnanosecond relaxation process and a slower process with a relaxation time of 1.5 or 5.6 ns at low or high ionic strength, respectively (16). The subnanosecond process

TABLE 2 **Secondary structure of peptide 1 in water, as determined from the Raman amide I band. For comparison, the secondary structure of melittin and of polyglycine in water is included (data taken from reference 15)**

		H_o	H_d	S_a	S_p	T	U	H_{tot}	S_{tot}	T + U
Peptide 1	%	64.7	33.7	−4.3	−5.0	8.1	2.8	98.4	−9.3	10.9
	Res	17	9	−1	−1	2	0	26	−2	2
Melittin	%	58.5	17.8	8.0	−1.3	8.4	8.6	76.3	6.7	17.0
(low salt)	Res	15	5	2	0	2	2	20	2	4
Melittin	%	68.5	23.8	−15.1	7.2	7.4	8.1	92.3	−7.9	15.5
(high salt)	Res	18	6	−4	2	2	2	24	−2	4
Polyglycine	%	79.0	19.8	−15.0	0.2	8.1	7.9	98.8	−14.8	16.0

Abbreviations: H_o = ordered helix, H_d = disordered helix, S_a = antiparallel strand, S_p = parallel strand, T = turn, U = undefined, $H_{tot} = H_o + H_d$, $S_{tot} = S_a + S_p$.

of melittin was interpreted as orientational fluctuations of the Trp side chain relative to the backbone, and the slow process as rotational diffusion of the monomer or the tetramer at low or high ionic strength, respectively. Adopting the same interpretation for peptide 1, the relaxation time of 1.8 ns would indicate slower fluctuations of the Trp side chain compared to melittin, and the relaxation time of 78 ns a much stronger aggregation, even at low ionic strength. In simplest approximation, considering the aggregate as a sphere, the relaxation time for rotational diffusion is proportional to the volume V of the sphere, $\Phi = \eta V/kT$ with η denoting the viscosity of the surrounding medium. Since for monomeric melittin the rotational relaxation time was 1.5 ns, the aggregation number of peptide 1 would follow as 78/1.5 = 52. However, smaller numbers may be obtained for a nonspherical shape of the aggregate. For a disc-like shape with an axial ratio of 3, one would obtain a value of 35 (19).

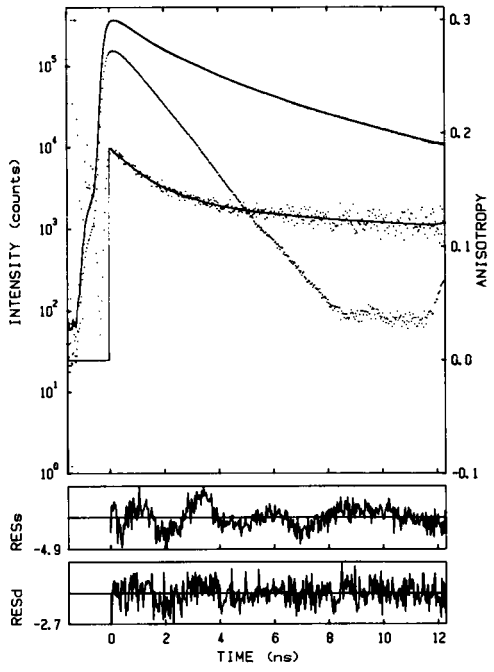

FIGURE 2 Intensity and anisotropy of the Trp fluorescence of 20 μM peptide 1 in buffer at 19°C. The experimental data including the fluorescence standard are shown (· · ·) together with the fits (——) and the residuals. The intensity was fitted by three exponentials and the anisotropy by two exponentials.

FAD measurements on peptide 1 in vesicle membranes

The intensity and anisotropy of the Trp fluorescence of peptide 1 in vesicle membranes of DMPC at a molar ratio of 1/150 is shown in Fig. 3, for the temperatures 19° and 36°C, i.e., below and above the lipid phase transition at 24°C. Since by analogy to melittin a slow relaxation process in the range of tens of ns was expected (16), the time window was extended to 60 ns and the measuring time to 12 h. Indeed, the anisotropy decreases over this time range, suggesting the existence of such a slow process. The results of fits of the intensity and the anisotropy are listed in Table 4.

The intensity involves three lifetimes that closely agree with those found for peptide 1 in water. In addition, however, a fourth lifetime of about 20 ns appears, although with a very small amplitude. The intensity at $t > 30$ ns is dominated by this slow component. A similar behavior has been observed for melittin in vesicle membranes (16). There, the long lifetime was about 10 ns.

When the anisotropy at 36°C was fitted in the usual way by two relaxation times and a residual anisotropy, the residual anisotropy was obtained as $r_\infty = -1.6$. This value lies outside the physical range of r_∞, extending

TABLE 3 **Results of fits of the intensity and anisotropy of the Trp fluorescence of peptide 1 in buffer (data shown in Fig. 2)**

τ_1 (ns), α_1	0.51 ± 0.01	0.411 ± 0.002
τ_2 (ns), α_2	1.89 ± 0.03	0.429 ± 0.007
τ_3 (ns), α_3	5.40 ± 0.06	0.159 ± 0.005
$\bar{\tau}$ (ns)	1.88	
χ_a^2	3.03	
Φ_1 (ns), b_1	1.8 ± 0.3	0.056 ± 0.002
Φ_2 (ns), b_2	78 ± 11	0.137 ± 0.001
r_∞		0.0 (fixed)
r_0		0.193
$\bar{\Phi}$ (ns)	56	
χ_d^2	1.03	

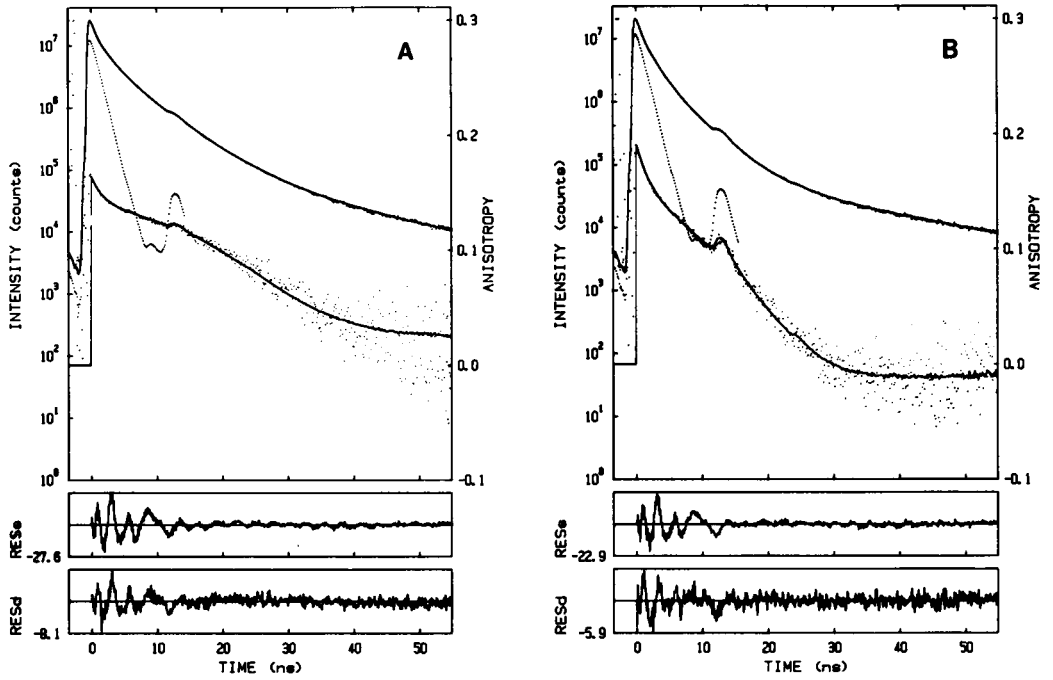

FIGURE 3 Intensity and anisotropy of the Trp fluorescence of peptide 1 in vesicle membranes of DMPC at a molar ratio of 1:150 and 19°C (*A*) or 36°C (*B*). The experimental data including the fluorescence standard are shown (· · ·) together with the fits (——) and the residuals. The intensity was fitted by four exponentials and the anisotropy by two exponentials and a residual anisotropy according to Eq. 6.

from 0.4 to −0.2. Therefore, as in the case of melittin (16), another fit was performed, permitting the emission dipole moment of the long lifetime component to differ in direction from the dipole moments of the three shorter lifetime components. With this additional degree of freedom, a reasonable fit could be obtained. The angle Θ_{es} between the emission dipole moment of the long lifetime component and the symmetry axis of the fluorophore became 59°, so that the Legendre polynomial becomes negative, $P_2(\cos\Theta_{es}) = -0.11$, leading to the negative anisotropy at long times. For melittin, the corresponding angle was 44° and the Legendre polyno-

TABLE 4 Results of fits of the intensity and anisotropy of the Trp fluorescence of peptide 1 in vesicle membranes of DMPC at 19°C and 36°C (data shown in Fig. 3)

	19°C		36°C	
τ_1 (ns), α_1	0.493 ± 0.002	0.561 ± 0.001	0.543 ± 0.003	0.546 ± 0.002
τ_2 (ns), α_2	2.05 ± 0.01	0.273 ± 0.001	1.80 ± 0.01	0.318 ± 0.002
τ_3 (ns), α_3	5.25 ± 0.02	0.162 ± 0.001	4.18 ± 0.01	0.134 ± 0.002
τ_4 (ns), α_4	18.6 ± 0.2	0.0044 ± 0.0002	21.7 ± 0.1	0.0027 ± 0.0001
$\bar{\tau}$ (ns)	1.77		1.48	
χ_s^2	27.6		15.6	
Φ_1 (ns), b_1			1.41 ± 0.03	0.038 ± 0.001
Φ_2 (ns), b_2			307 ± 300	1.8 ± 2
r_∞				−1.6 ± 2
r_0				0.19
$\bar{\Phi}$ (ns)			301	
χ_d^2			2.74	
Φ_1 (ns), β_1	1.6 ± 0.9	0.068	1.9 ± 2	0.092
Φ_2 (ns), β_2	81 ± 11	0.157 ± 0.001	24 ± 8	0.184 ± 0.008
$\langle P_2 \rangle$, β_3	0.66	0.18 ± 0.10	0.56	0.12 ± 0.25
$P_2(\Theta_{ef})$, Θ_{ef}	0.43 ± 0.14	38°	0.50 ± 0.12	35°
$P_2(\Theta_{es})$, Θ_{es}	0.08 ± 0.20	52°	−0.11 ± 0.20	59°
r_∞		0.014		−0.013
r_o		0.171		0.200
$\bar{\Phi}$ (ns)	57		17	
χ_d^2	2.30		1.79	

mial positive, $P_2(\cos \Theta_{es}) = 0.26$. The two relaxation times result as 1.9 and 24 ns, and the orientational order parameter associated with the slow relaxation process as $\langle P_2 \rangle = 0.56$. These numbers are very similar to the results obtained for melittin (16). There, the slow relaxation process with 30 ns was interpreted as resulting from orientational fluctuations of the helices, and the fast relaxation process as resulting from fluctuations of the Trp side chains relative to the helix backbone. Applying the same assignment to peptide 1, the experimental results indicate that peptide 1 also performs helix fluctuations in membranes.

Similar results are obtained from fits of the anisotropy at 19°C. The main difference is that here $P_2(\cos \Theta_{es})$ is positive, implying the residual anisotropy to remain positive. Furthermore, the slow relaxation process becomes even slower, $\Phi_2 = 81$ ns, and the associated order parameter higher, $\langle P_2 \rangle = 0.66$. These results indicate a partial immobilization of peptide 1 in the ordered lipid phase. For melittin, the long relaxation time did not vary upon passing through the lipid phase transition.

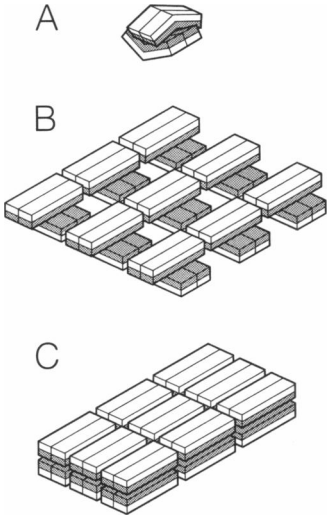

FIGURE 4 Schematic representation of the tetramer of melittin (*A*) and of possible oligomers formed by peptide 1 (*B* and *C*). Rectangles represent amphiphilic helices with hydrophobic (*dotted*) and hydrophilic (*white*) surfaces. In the case of oligomers, bilayers might be formed with the pairs of antiparallel helices oriented either perpendicular (*B*) or parallel (*C*).

DISCUSSION

Peptide 1 was found to share many of the structural and dynamic properties of melittin. This is not surprising, since peptide 1 was designed as an amphiphilic α-helix analogous to melittin, with the identical charged segment at the COOH terminus. At the same time, however, peptide 1 exhibits some distinct differences from melittin: In water, peptide 1 (*i*) has a higher α-helix content; (*ii*) is more strongly aggregated, even at low ionic strength; and (*iii*) has less motional freedom of the Trp side chains. Additionally, in vesicle membranes below the lipid phase transition, peptide 1 is more strongly immobilized than melittin.

Attempting to interpret these differences, we focus on the role of the single proline residue present in melittin at position 14 and absent in peptide 1. This proline residue is likely to cause the kink in the melittin helix, while the helix of peptide 1 should be straight. Both kinds of helixes may associate in antiparallel pairs and such pairs may pack on top of each other to shield their hydrophobic sides from water. For kinked helixes, however, the pairs have to pack crosswise and only two pairs can pack favorably, leading to the tetramer of melittin (Fig. 4 *A*). For straight helixes, as in the case of peptide 1, there appears to be no such restriction in aggregation, and large two-dimensional peptide bilayers may be formed (Fig. 4 *B* and *C*). Whether the orientation of the helix pairs in the two layers is parallel or perpendicular will depend on details of the interaction, but a parallel orientation seems to be more favorable (Fig. 4 *C*). Different shapes of the peptide bilayers may also be envisaged, ranging from disc-like to rod-like. In any case, however, the stronger aggregation of peptide 1 seems to be interpretable as a consequence of the straight helix and, thus, the absence of the proline residue.

A dense packing of the helixes in a peptide bilayer may also explain the other structural and dynamical differences between peptide 1 and melittin mentioned above. The absence of Pro14 in peptide 1 certainly increases the α-helix content. This effect, however, does not seem to be large enough to yield an α-helix content of nearly 100%. Presumably, the COOH-terminal segment has to become α-helical in addition. For melittin, this has been shown to occur at high ionic strength, where the electrical charges of the COOH terminus are shielded (Table 2). For peptide 1, this may be achieved by a dense packing in the peptide bilayer. In an analogous manner, this packing may reduce the motional freedom of the Trp side chains.

The reduction of the mobility of peptide 1 in membranes below the lipid phase transition indicates a strong interaction of the peptide with the ordered lipids. The simplest interpretation would be to postulate that on passing through the phase transition the peptide changes its position from that of lying flat on the membrane to being inserted into the membrane, presumably in a membrane-spanning manner. Incorporated in the membrane, it would be strongly immobilized by the ordered lipids. Melittin, on the other hand, behaves differently and does not become immobilized below the lipid phase transition (16). One would then conclude that melittin does not insert into the membrane below the lipid phase transition. The reason for that may again lie in the shape of the helix. The kinked helix of melittin may be expelled from the ordered lipids, while the straight helix of pep-

tide 1 may be tolerated. In addition, peptide 1 contains a longer stretch of uncharged residues than melittin, which also may facilitate insertion into the membrane. Further studies on the position and orientation of the two peptides are required to clarify this point. But it seems as if all the differences in the structural and dynamical behavior of peptide 1 and melittin may be traced back to the absence or presence of the single proline residue in the middle of the helix and the resulting shape of the helix, straight or kinked.

If this is true, the analogue P14A should behave similarly to peptide 1, and the same should hold for δ-hemolysin, which also contains an amphiphilic helix without a proline (Table 1). P14A was shown by NMR measurements to form regular α-helixes (14), but information on the aggregation state in water is not available. δ-Hemolysin, however, was found to form large oligomers in water, with an aggregation number of about 70 (20), very similar to peptide 1. Concerning the dynamic properties, the NMR data indicate that the helix of P14A is more rigid around residue 14 than the melittin helix (14). The same behavior would be expected for peptide 1. The difference in rigidity between P14A or peptide 1 and melittin, however, does not extend up to Trp19, therefore it is not astonishing that the Trp fluctuations are rather similar for peptide 1 and melittin.

Finally, one may try to correlate the structural and dynamic differences between peptide 1 and melittin with their functional differences. Peptide 1 was found to be more effective in hemolysis than melittin (3). We propose, as a hypothesis, an interpretation of this effect within the framework of the "raft" model (11). Within this model it is essential that large monolayers of peptide, the "rafts," form at the membrane surface. Peptide 1 aggregating in large oligomers, possibly bilayers, should also be able to form "rafts" and therefore be very effective in hemolysis. Melittin, on the other hand, aggregates in tetramers, thus should be less prone to form "rafts" and be less effective in hemolysis.

The behavior of the analogue P14A and of δ-hemolysin is compatible with this hypothesis. Both are expected to form straight helixes and, therefore, rafts, thus implying a strong hemolytic effect as indeed observed (14, 20).

Unfortunately, the ion channel activity of peptide 1 is not known. For the analogue P14A, however, which in every respect seems to behave like peptide 1, this activity was reduced in comparison to melittin (14). This was interpreted as a consequence of the straight helixes of P14A. In the ion channel structure, which presumably involves a transmembrane arrangement and aggregation of the helixes, straight helixes would bring the highly charged COOH-terminal segments closer to each other and thus would destabilize the channel. Likewise, micellization was found to be slowed down for P14A, hence also in micellization straight helixes are less effective than kinked helixes.

In summary, melittin, peptide 1, P14A, and δ-hemolysin all may form amphiphilic helixes. Therefore, they all are soluble in water upon aggregation and, at the same time, are able to associate with membranes. Melittin forms kinked helixes due to a proline residue at position 14 and, therefore, aggregates in tetramers, while the other three peptides lacking this proline residue form straight helixes and aggregate in large oligomers. They all induce ion channel activity, hemolysis, and micellization of membranes, but with different efficiencies. The kinked helixes of melittin are more effective in inducing ion channel activity and micellization, while the straight helixes of the other peptides are more effective in hemolysis. Thus, by playing with one proline residue, one can optimize one or the other activity in this family of peptides.

Received for publication 20 May 1992 and in final form 7 August 1992.

REFERENCES

1. Fukushima, D., J. P. Kupferberg, S. Yokoyama, D. J. Kroon, E. T. Kaiser, and F. J. Kézdy. 1979. A synthetic amphiphilic helical docosapeptide with the surface properties of plasma apolipoprotein A-I. *J. Am. Chem. Soc.* 101:3703–3704.
2. Yokoyama, S., D. Fukushima, F. J. Kézdy, and E. T. Kaiser. 1980. The mechanism of activation of lecithin: cholesterol acyltransferase by apolipoprotein A-I and an amphiphilic peptide. *J. Biol. Chem.* 255:7333–7340.
3. DeGrado, W. F., F. J. Kézdy, and E. T. Kaiser. 1981. Design, synthesis and characterization of a cytotoxic peptide with melittin-like activity. *J. Am. Chem. Soc.* 103:679–681.
4. DeGrado, W. F., G. F. Musso, M. Lieber, E. T. Kaiser, and F. J. Kézdy. 1982. Kinetics and mechanism of hemolysis induced by melittin and by a synthetic melittin analogue. *Biophys. J.* 37:329–338.
5. Dempsey, C. E. 1990. The actions of melittin on membranes. *Biochim. Biophys. Acta.* 1031:143–161.
6. Terwilliger, T. C., L. Weissman, and D. Eisenberg. 1982. The structure of melittin in the form I crystals and its implication for melittin's lytic and surface activities. *Biophys. J.* 37:353–361.
7. Frey, S., and L. K. Tamm. 1991. Orientation of melittin in phospholipid bilayers. A polarized attenuated total reflection infrared study. *Biophys. J.* 60:922–930.
8. Stanislawski, B., and H. Rüterjans. 1987. ^{13}C-NMR investigation of the insertion of the bee venom melittin into lecithin vesicles. *Eur. Biophys. J.* 15:1–12.
9. Altenbach, C., and W. L. Hubbell. 1988. The aggregation state of spin-labeled melittin in solution and bound to phospholipid membranes: Evidence that membrane-bound melittin is monomeric. *Proteins.* 3:230–242.
10. John, E., and F. Jähnig. 1991. Aggregation state of melittin in lipid vesicle membranes. *Biophys. J.* 60:319–328.
11. Raghunathan, G., P. Seetharamulu, B. R. Brooks, and H. R. Guy. 1990. Models of δ-hemolysin membrane channels and crystal structures. *Proteins.* 8:213–225.
12. Dufourc, E. J., J. F. Faucon, G. Fourche, J. Dufourcq, T. Gulik-Krzywicki, and M. le Maire. 1986. Reversible disc-to-vesicle

transition of melittin-DPPC complexes triggered by the phospholipid acyl chain melting. *FEBS (Fed. Eur. Biochem. Soc.) Lett.* 201:205–209.

13. Dempsey, C. E., and B. Sternberg. 1991. Reversible disc-micellization of dimyristoylphosphatidylcholine bilayers induced by melittin and [Ala-14]melittin. *Biochim. Biophys. Acta.* 1061:175–184.
14. Dempsey, C. E., R. Bazzo, T. S. Harvey, I. Syperek, G. Boheim, and I. D. Campbell. 1991. Contribution of proline-14 to the structure and actions of melittin. *FEBS (Fed. Eur. Biochem. Soc.) Lett.* 281:240–244.
15. Vogel, H., and F. Jähnig. 1986. The structure of melittin in membranes. *Biophys. J.* 50:573–582.
16. John, E., and F. Jähnig. 1988. Dynamics of melittin in water and membranes as determined by fluorescence anisotropy decay. *Biophys. J.* 54:817–827.
17. Williams, R. W. 1983. Estimation of protein secondary structure from the laser Raman amide I spectrum. *J. Mol. Biol.* 166:581–603.
18. Lakowicz, J. R., G. Laczko, I. Gryczynski, and H. Cherek. 1986. Measurement of subnanosecond anisotropy decays of protein fluorescence using frequency-domain fluorometry. *J. Biol. Chem.* 261:2240–2245.
19. Memming, R. 1961. Theorie der Fluoreszenzpolarisation für nicht kugelsymmetrische Moleküle. *Z. Phys. Chem.* 28:168–189.
20. Kantor, H. S., B. Temples, and W. V. Shaw. 1972. Staphylococcal delta hemolysin: Purification and characterization. *Arch. Biochem. Biophys.* 151:142–156.